Article

Not peer-reviewed version

A decrease in ciliary motility induced by a CO2/HCO3--free solution characteristic of ciliated human nasal epithelial cells: acceleration of HCO3- transport by carbonic anhydrase IV

Shota Okamoto , Makoto Yasuda * , Kotoku Kawaguchi , Kasane Yasuoka , Yumi Kikukawa , Shinji Asano , Taisei Tsujii , Sana Inoue , Kikuko Amagase , Taka-aki Inui , Shigeru Hirano , Toshio Inui , Yoshinori Marunaka , Takashi Nakahari *

Posted Date: 28 June 2024

doi: 10.20944/preprints202406.2013.v1

Keywords: nasal cilia; intracellular pH; NH4+ pulse; NBC; bicarbonate transport metabolon; airway; ALI; ciliary motility; ciliary waveform; CBF

 doi:10.20944/preprints202406.2013.v1

Article

A decrease in Ciliary Motility Induced by a CO_2/HCO_3^--Free Solution Characteristic of Ciliated Human Nasal Epithelial Cells: Acceleration of HCO_3^- Transport by Carbonic Anhydrase IV

Shota Okamoto [1,2,*]Makoto Yasuda [2], Kotoku Kawaguchi [1,3], Kasane Yasuoka [1,3], Yumi Kikukawa [1,3], Shinji Asano [1,3], Taisei Tsujii [1,4], Sana Inoue [4], Kikuko Amagase [4], Taka-aki Inui [2], Shigeru Hirano [2], Toshio Inui [5] and Yoshinori Marunaka [1,6,*]Takashi Nakahari [1,6]

[1] Research Laboratory for Epithelial Physiology, Research Organization of Science and Technology, BKC Ritsumeikan University, Kusatsu 525-8577, Japan; ymr18005@fc.ritsumei.ac.jp
[2] Department of Otolaryngology-Head and Neck Surgery, Graduate School of Medical Science, Kyoto Prefectural University of Medicine, Kyoto 602-8566, Japan; okmt721@koto.kpu-m.ac.jp, inui1227@koto.kpu-m.ac.jp, hirano@koto.kpu-m.ac.jp
[3] Laboratory of Molecular Physiology, Faculty of Pharmacy, Ritsumeikan University BKC, Kusatsu 525-8577, Japan; kasane.yasuoka@gmail.com, coconut2110@gmail.com, k-kawagu@dent.meikai.ac.jp, ashinji@ph.ritsumei.ac.jp
[4] Laboratory of Pharmacology and Pharmacotherapeutics, Faculty of Pharmacy, Ritsumeikan University BKC, Kusatsu 525-8577, Japan; ph0161vh@ed.ritsumei.ac.jp, sinoue@fc.ritsumei.ac.jp, amagase@ph.ritsumei.ac.jp
[5] Saisei Mirai Clinics, Moriguchi 570-0012, Japan; t-inui@saisei-mirai.or.jp
[6] Medical Research Institute, Kyoto Industrial Health Association, Kyoto 604-8472, Japan; marunaka@koto.kpu-m.ac.jp
* Correspondence: nakahari@fc.ritsumei.ac.jp; myasu@koto.kpu-m.ac.jp; Tel.: +81 775 61 2655; +81 75 251 5603

Abstract: An application of CO_2/HCO_3^--free solution (Zero-CO_2) did not increase intracellular pH (pH_i) in ciliated human nasal epithelial cells (c-hNECs), leading to no increase in the beating frequency (CBF) or bend distance (CBD, an index of amplitude). This study demonstrated that the pH_i of the c-hNECs expressing carbonic anhydrase IV (CAIV) is high (7.64), while that of the ciliated human bronchial epithelial cells (c-hBECs) expressing no CAIV is low (7.10). Upon applying Zero-CO_2, an extremely high level of pH_i caused the pH_i, CBF and CBD to decrease, while a low level of pH_i caused them to increase. The high pH_i was generated by a high rate of HCO_3^- influx via interactions between CAIV and Na^+/HCO_3^- cotransport (NBC) in c-hNECs. An NBC inhibitor (S0859) decreased the pH_i and CBF, and Zero-CO_2 application increased the CBF in S0859-treated c-hNECs. In conclusion, the interactions of CAIV and NBC maximize the HCO_3^- influx to increase the pH_i in c-hNECs. This novel mechanism causes the pH_i to decrease, leading to no increase in CBF and CBD in c-hNECs upon Zero-CO_2 application, and appears to play a crucial role in maintaining pH_i, CBF and CBD in c-hNECs periodically exposed to air (0.04% CO_2) with respiration.

Keywords: nasal cilia; intracellular pH; NH_4^+ pulse; NBC; bicarbonate transport metabolon; airway; ALI; ciliary motility; ciliary waveform; CBF

1. Introduction

Ciliated human nasal epithelial cells (c-hNECs) have been differentiated from human nasal epithelia (operation samples) using air–liquid interface (ALI) culture. Inhaled small particles, such as chemicals, allergens, bacteria and viruses, are trapped by the surface mucous layer of the nasal epithelium and swept away from the nasal cavity by the beating cilia [1–4]. Impairment of the nasal

 doi:10.20944/preprints202406.2013.v1

beating cilia, such as primary ciliary dyskinesia, causes sinusitis [1,2,4]. Thus, beating cilia play a crucial role in maintaining a healthy nasal cavity [1,3,4,7]. Activities of the airway beating cilia are controlled by various substances, such as cAMP, cGMP, Ca^{2+}, H^+ and Cl^- [2,4–10]. Among them, the H^+ is an important regulator of airway beating cilia; an increase in intracellular pH (pH_i) enhances the ciliary beat frequency (CBF) and ciliary bend distance (CBD, an index of ciliary beat amplitude (CBA)); contrarily, a decrease in pH_i suppresses them [6,8–10].

The ciliated nasal epithelium is a special tissue, the apical surface of which is periodically exposed to fresh air with respiration. The temperature and CO_2 concentration of air are different from those of gas existing in the trachea and lung airways. The c-hNECs have been shown to express thermosensitive transient receptor potentials (TRP) A1 and M8, which keep the ciliary beating at an adequate level in cooled air [11]. Moreover, the CO_2 concentration (0.04%) of air is significantly lower than that of blood or interstitial fluid (5%). Periodic air exposure (0.04% CO_2) appears to increase the pH_i, leading to a CBF increase, as shown in tracheal and lung airway ciliated cells upon applying the CO_2/HCO_3^--free solution (Zero-CO_2) [8–10]. However, a previous study demonstrated that the application of Zero-CO_2 does not increase the pH_i, CBF or CBD in c-hNECs [6]. Moreover, the application of NH_4^+ pulse induced gradual decreases in pH_i and CBF following their immediate increases. The gradual decreases in pH_i and CBF were inhibited by acetazolamide (a carbonic anhydrase (CA) inhibitor) [6]. These findings indicate that H^+ is produced from CO_2 by the CA-mediated reaction (Eq. 1), even during the application of Zero-CO_2 in c-hNECs.

$$CO_2 \leftrightarrow H^+ + HCO_3^- \text{ (Eq. 1)}$$

However, the factors, which shift the Eq. 1 to the right (H^+ production) upon applying Zero-CO_2 or the NH_4^+ pulse, remain unidentified in c-hNECs.

A previous study showed that carbonic anhydrase IV (CAIV) is expressed in nasal epithelia [12,13]. However, the role of CAIV is not fully understood in nasal epithelia, especially in beating cilia. Previous studies have also demonstrated that CAIV interacts with Na^+-HCO_3^- cotransporter (NBC) in HEK293 cells transfected with CAIV and NBC [14], renal proximal tubules [15] and retinal epithelium [16]. Nasal epithelia have also been shown to express NBC [17]. CAIV may interact with NBC in c-hNECs.

We hypothesized that the interactions between CAIV and NBC maximize the rate of HCO_3^- influx in c-hNECs, leading to a high pH_i. The high pH_i (low $[H^+]_i$) may shift the Eq.1 to the right, inducing no increase in CBF or CBD, even upon applying Zero-CO_2, and inducing their gradual decreases during application of the NH_4^+ pulse. We also used ciliated human bronchial epithelial cells (c-hBECs), which were differentiated from normal human bronchial epithelial cells (NHBE) using ALI culture [18]. We found that c-hBECs, similar to c-hNECs, express CAs except CAIV, NBCs and anion exchangers (AEs). The c-hBECs appear to provide a good model of airway ciliated cells expressing no CAIV. The goal of this study is to clarify the CAIV-mediated mechanism, which suppresses increases in CBF, CBD and pH_i in c-hNECs upon applying Zero-CO_2.

2. Result

2.1. Expression of CA

2.1.1. PCR

The mRNA expressions of CA subtypes (I, II, III, IV and Vb) were examined in c-hNECs and c-hBECs using Reverse Transcription-Polymerase Chain Reaction (RT-PCR, Figure 1A,B). The primers used are shown in Table 1. CAI, CAII, CAIII, CAIV and CAVb mRNA were expressed in c-hNECs (Figure 1A), whereas CAI, CAII, CAIII and CAVb mRNA, but not CAIV mRNA, were expressed in c-hBECs (Figure 1B). The expression levels of CAIV mRNA were examined in c-hNECs and c-hBECs using Real-Time PCR (Figure 1C). The expression levels of CAIV mRNA were significantly higher in c-hNECs than in c-hBECs.

 doi:10.20944/preprints202406.2013.v1

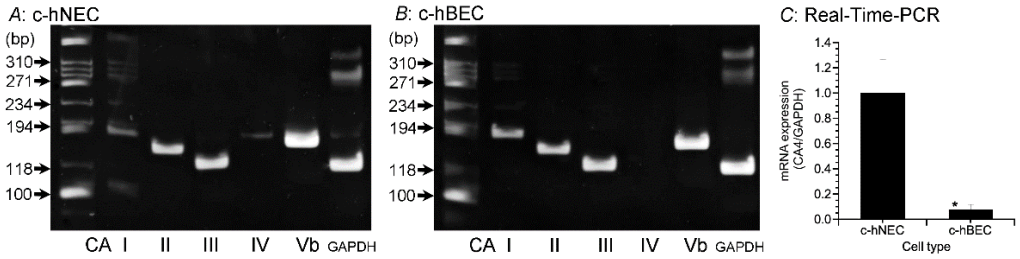

Figure 1. Expression of CA mRNA. The expressions of CAI, CAII, CAIII, CAIV, and CAVb were examined using RT-PCR. (**A)** c-hNECs. (**B)** c-hBECs. CAIV was expressed in c-hNECs, but not in c-hBECs. (**C**) The Real-Time PCR examination of CAIV mRNA in c-hNECs and c-hBECs. The expression level of CAIV mRNA was significantly higher in c-hNEC than in c-hBECs. * indicates significant difference ($p < 0.01$).

Table 1. Primers used to amplify CA.

Transcript	Direction	Sequence	Size (bp)
CA1	Sense	AGCTGCCTCAAAGGCTGATG	181
	Antisense	GGTCCAGAAATCCAGGGATGAA	
CA2	Sense	TTACTGGACCTACCCAGGCTCAC	167
	Antisense	GCCAGTTGTCCACCATCAGTTC	
CA3	Sense	CATGAGAATGGCGACTTCCAGA	141
	Antisense	GAATGAGCCCTGGTAGGTCCAGTA	
CA4	Sense	TCCCTAGAAACCTAGGGTCATTTCA	156
	Antisense	TGGAGCTAGATCACGTTTCACAA	
CA5b	Sense	TGTTCTGAAGTGAAAGTCTGGTCTG	172
	Antisense	CCAAACTAGAGTGCCCTGGATG	

The expression of five CA subtypes (I, II, III, IV, and Vb) was examined in two cell types of c-hNECs (uncinate process and nasal polyp) of chronic sinusitis (CS) patients, and both types of c-hNECs expressed five CA subtypes.

2.1.2. Western Blotting

The expression of CAIV protein was examined using Western blotting (WB) in c-hNECs and c-hBECs. In this study, AF2186 (R&D System) anti-CAIV antibody was used. CAIV is known to have two N-glycosylation sites, the sialations of which increase the molecular mass by 11–45 kDa [19]. The specific band for CAIV has been shown to be approximately 33–40 kDa (datasheet of AF2186 supplied from R&D systems, Minneapolis, MN, USA), and previous studies demonstrated that the band for CAIV is 46 kDa in HEK293 cells co-transfected with cDNA encoding AE2, CAII and CAIV [14,20]. Therefore, we treated the lysate with PNGaseF (Roche, Basel, Switzerland) overnight before starting the Western blotting. In the Western blotting, a single band was detected at 40 kDa in c-hNECs. However, in c-hBECs, the CAIV band was faint (Figure 2A). The densities of the CAIV band were normalized by those of GAPDH. The normalized value of CAIV protein expression was significantly higher in c-hNECs ($n = 4$) than in c-hBECs ($n = 4$) ($p < 0.01$) (Figure 2B).

 doi:10.20944/preprints202406.2013.v1

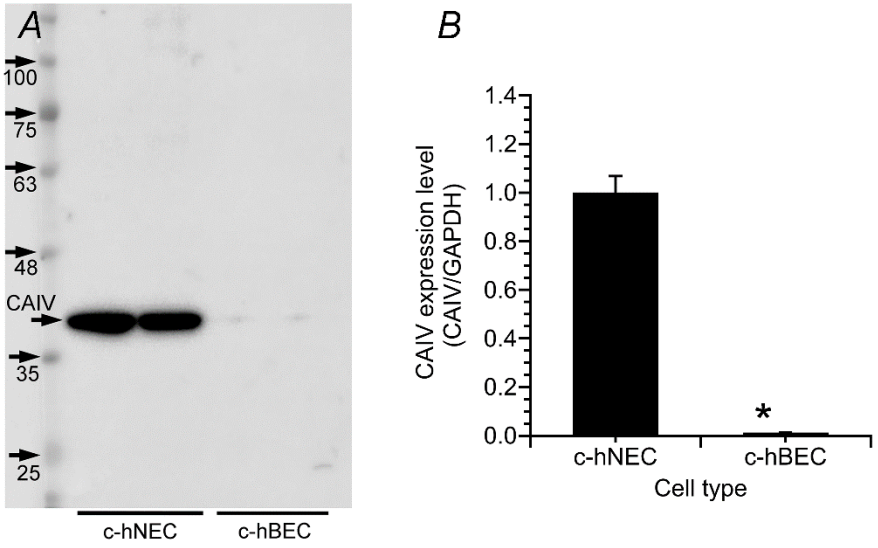

Figure 2. Western blotting for CAIV in c-hNECs and c-hBECs. **(A)** The single band of CAIV (40 kDa) was detected in c-hNECs but was faint in c-hBECs. **(B)** Densitometric analysis. The expression of CAIV protein was higher in c-hNECS (n = 4) than in c-hBECs (n = 4). * indicates significant difference ($p < 0.01$).

2.1.3. Immunofluorescence Examination for CAIV

Immunofluorescence examinations for CAIV were carried out in c-hNECs (Fifure 3A) and c-hBECs (Figure 3B) using AF2186 (a CAIV antibody, R&D Systems). In c-hNECs, cilia were positively stained for CAIV (Figure 3A1). Staining for AC-tubulin (a cilia marker) clearly shows cilia on the apical surface of c-hNECs (Figure 3A2). In the merged image (Figure 3A3), nuclei were stained using DAPI, and cilia are positively stained for both CAIV and AC-tubulin. Figure 3A4 shows the phase contrast image of c-hNECs. In c-hBECs, no immunofluorescence for CAIV was detected in cilia (Figure 3B1). Cilia were positively stained for AC-tubulin (Figure 3B2). In the merged image (Figure 3B3), nuclei were stained with DAPI and cilia were stained with AC-tubulin. Figure 3B4 shows the phase contrast image of c-hBECs. Immunofluorescence examination revealed that CAIV exists in apical cilia of c-hNECs, but not in those of c-hBECs.

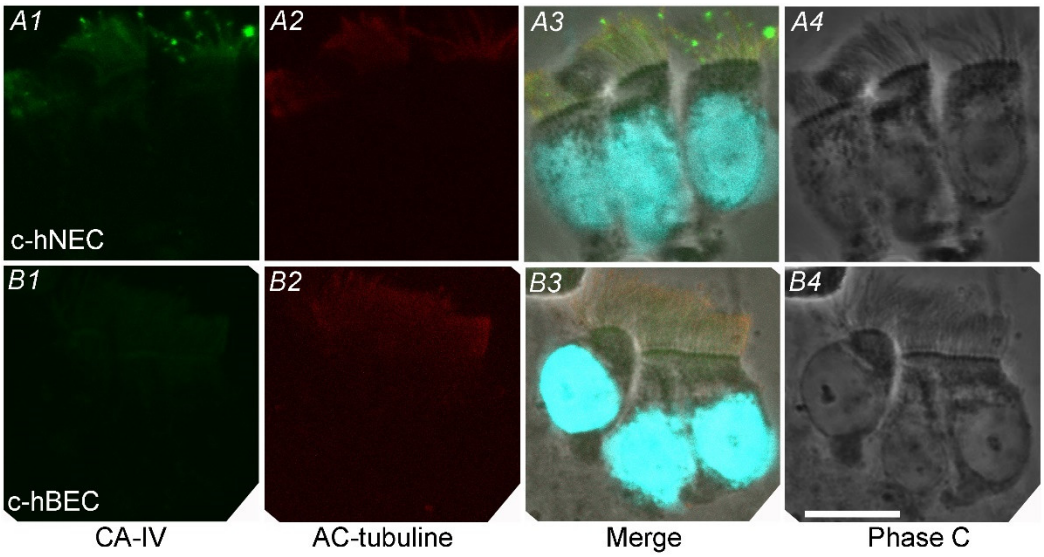

 doi:10.20944/preprints202406.2013.v1

Figure 3. Immunofluorescence examination for CAIV. **(A)** c-hNEC. **A1**: CAIV, **A2**: AC-tubulin (a cilia marker), **A3**: merged image, **A4**: phase contrast image. The cilia of c-hNEC were immunopositively stained for CAIV. **(B)** c-hBEC. **B1**: CAIV, **B2**: AC-tubulin, **B3**: merged image, **B4**: phase contrast image. The cilia of c-hBECs were not stained for CAIV.

2.2. Expression of NBC and AE

The mRNA expression of NBC subtypes (NCBE (SLC4A10), NBC1 (SLC4A11), NBCe1 (SLC4A4), NBCe2 (SLC4A5), NBCn1 (SLC4A7) and NDCBE1 (SLC4A8)) was examined using RT-PCR in c-hNECs (Figure 4A) and c-hBECs (Figure 4B). The mRNA expressions of NBC1, NBCe1, NBCe2, NBCn1 and NDCBE1, but not NCBE, were detected in both c-hNECs and c-hBECs. The mRNA expression of AE subtypes (SLC26A4, SLC26A6, SLC26A9, SLC4A2 (AE2) and SLC4A3 (AE3)) was also examined using RT-PCR in c-hNECs (Figure 4C) and c-hBECs (Figure 4D). The mRNA expression of AE2 was detected in c-hNECs and c-hBECs, whereas the mRNA expression of SLC26A4, SLC26A6, SLC26A9 or AE3 was not. There was no difference in the expression of NBCs or AEs between c-hNECs and c-hBECs. The expressions of NBC and AE subtypes were also examined in c-hNECs from two types of tissue samples (uncinate process and nasal polyp) from CS patients. The expressions of mRNA of NBC1, NBCe1, NBCe2, NBCn1, NDCBE1 and AE2 were similar in both cell types of c-hNECs. The primers used for detecting NBC and AE are shown in Table 2.

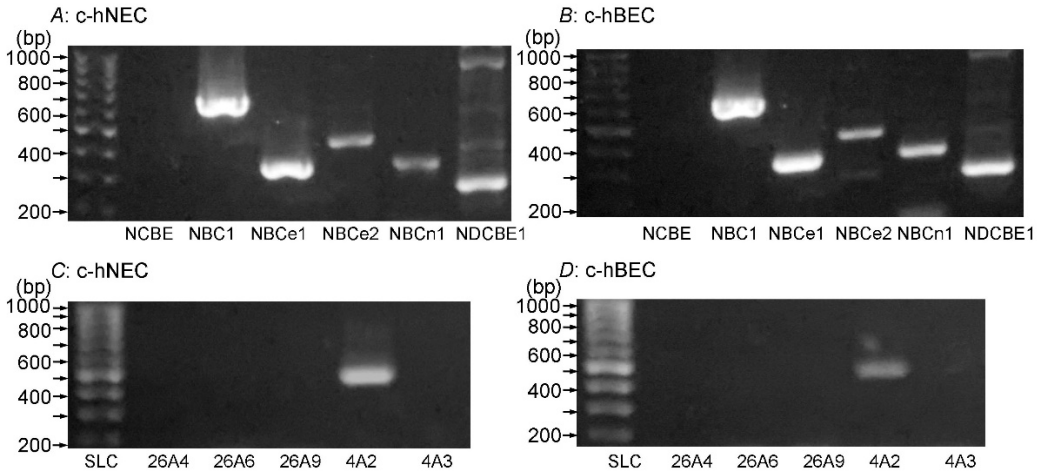

Figure 4. NBC expression (**A,B**) and AE expression (**C, D**) in c-hNECs and c-hBECs. The mRNA of both HCO_3^- transporters was detected using RT-PCR. (**A**) c-hNECS. NBC1, NBCe1, NBCe2 and NBCn1, but not NCBE, were expressed. (**B**) c-hBECs. NBC1, NBCe1, NBCe2 and NBCn1, but not NCBE, were expressed. **(C)** c-hNECs. SLC4A2 was expressed, but SLC26A4, SLC26A6, SLC26A9 and SLC4A3 were not. (**D**) c-hBECs. SLC4A2 was expressed, but SLC26A4, SLC26A6, SLC26A9 and SLC4A3 were not. There is no difference in the mRNA expression of NBCs or AEs between c-hNECs and c-hBECs.

Table 2. Primers used to amplify NBCs and AEs.

NBC			
Transcript	Direction	Sequence	Size (bp)
NCBE (SLC4A10)	Sense	GCAGGTCAGGTTGTTTCTCCTC	498
	Antisense	TCTTCCTCTTCTCCTGGGAAGG	
NBC1 (SLC4A11)	Sense	GGCCTGTGGAACAGTTTCTTCC	690
	Antisense	TGCCCTTCACCAGCCTGTTCTC	
NBCe1 (SLC4A4)	Sense	GGTGTGCAGTTCATGGATCGTC	336
	Antisense	GTCACTGTCCAGACTTCCCTTC	
NBCe2 (SLC4A5)	Sense	ATCTTCATGGACCAGCAGATCAC	468
	Antisense	TGCTTGGCTGGCATCAGGAGG	

 doi:10.20944/preprints202406.2013.v1

NBCn1 (SLC4A7)	Sense	CAGATGCAAGCAGCCTTGTGTG	328
	Antisense	GGTCCATGATGACCACAAGCTG	
NDCBE1 (SLC4A8)	Sense	GCTCAAGAAAGGCTGTGGCTAC	243
	Antisense	CATGAAGACTGAGCAGCCCATC	
AE			
AE2	Sense	GAAGATTCCTGAGAATGCCT	181
	Antisense	GTCCATGTTGGCAGTAGTCG	
AE3	Sense	ATCTGAGGCAGAACCTGTGG	418
	Antisense	TTTCACTAAGTGTCGCCGC	
SLC26A4	Sense	GTTTACTAGCTGGCCTTATATTTGGACTGT	484
	Antisense	AGGCTATGGATTGGCACTTTGGGAACG	
SLC26A6	Sense	TAGGGGAGGTTGGGCCAGGGATGC	456
	Antisense	TGCCGGGAAGTGCCAAACAGGAAGAAGTAGAT	
SLC26A9	Sense	TCCAGGTCTTCAACAATGCCAC	400
	Antisense	CGAGTCTTGTGCATGTAGCGAG	

2.3. CBF and CBD in c-hNECs and c-hBECs

In c-hNECs, the ciliary beat frequency (CBF) was 8.39 ± 2.44 Hz (n = 47) and the ciliary bend distance (CBD) was 54.0 ± 27.2 μm (n = 11) in c-hNECs. There was no difference in CBFs among two cell types of CS patients. In c-hBECs, the CBF was 8.37 ± 1.04 Hz (n = 12) and the CBD was 65.3 ± 8.0 μm (n = 12). There was no difference in CBF or CBD between c-hNECs and c-hBECs.

2.3.1. Ciliated-hNECs

2.3.1.1. Effects of CO_2/HCO_3^- -free solution (Zero-CO_2) on CBF, CBD and pH_i in c-hNECs

Figure 5A shows changes in CBF and CBD ratios in c-hNECs upon applying Zero-CO_2. The application of Zero-CO_2 induced a small transient increase followed by a gradual decrease in the CBF ratio or CBD ratio. The ratios of CBF and CBD 1.5 min after applying Zero-CO_2 were 1.02 (n = 15) and 1.01 (n = 11, $p < 0.05$), and those 10 min after the application were 0.91 and 0.88 ($p < 0.05$), respectively. Thus, the application of Zero-CO_2 decreased both CBF and CBD ratios in c-hNECs. Changes in the pH_i were measured by the fluorescence ratio of BCECF (F490/F440) (Figure 5B). The pH_i of c-hNECs in the control solution was 7.64 ± 0.19 (n = 9). The application of Zero-CO_2 gradually decreased the pH_i. The pH_i at 1 min after the application was 7.55 (n = 9) and that at 5 min after the application was 7.24. This result indicates that the application of Zero-CO_2 shifts the Eq. 1 to the right (H^+ production). A small amount of CO_2 is produced by metabolism in the Zero-CO_2, and the application of Zero-CO_2 decreases the intracellular HCO_3^- concentration ($[HCO_3^-]_i$) due to there being no HCO_3^- entry. A high pH_i (a low $[H^+]_i$) and a low $[HCO_3^-]_i$ may shift the Eq. 1 to the right. Inui et al. (2020) observed similar results in c-hNECs [6], although transient increases in CBF, CBD and pH_i were larger than those observed in this study. However, they were negligibly small compared with those reported by airway ciliated cells [6,8,9].

 doi:10.20944/preprints202406.2013.v1

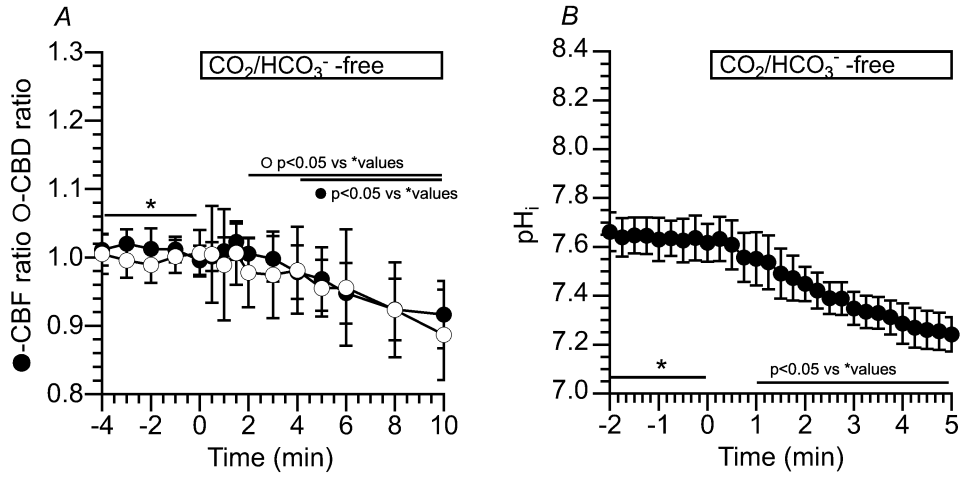

Figure 5. Changes in CBF, CBD and pH_i in c-hNECs upon applying the CO_2/HCO_3^--free solution (Zero-CO_2). **(A)** Changes in CBF and CBD ratios. Application of Zero-CO_2 induced a small transient increase followed by a gradual decrease in CBF or CBD. **(B)** Changes in pH_i. Application of Zero-CO_2 gradually decreased the pH_i from 7.65 to 7.30.

Changes in CBF and CBD ratios were similar upon applying Zero-CO_2. In this study, we used the CBF to compare the activities of ciliary beating throughout the experiments.

2.3.1.2. Effects of NH_4^+ Pulse on CBF, CBD and pH_i in c-hNECs

An NH_4^+ pulse was applied to increase the pH_i of c-hNECs in the Zero-CO_2. The switch to Zero-CO_2 slightly increased the CBF in this experiment, but the increase in CBF was not significant. Then, the application of NH_4^+ pulse induced an immediate increase followed by a gradual decrease in CBF. The ratios of CBF at 1 min and 5 min from the start of the NH_4^+ pulse were 1.09 (n = 6) and 1.03 (n = 6), respectively. Both values were significantly different ($p < 0.05$). The cessation of NH_4^+ pulse immediately decreased the CBF (Figure 6A). A previous study demonstrated that a gradual decrease in CBF during the NH_4^+ pulse is inhibited by acetazolamide (a CA inhibitor) [6]. These results suggest that the decrease in CBF during the application of the NH_4^+ pulse is induced by a pH_i decrease in c-hNECs. A high pH_i value and a low $[HCO_3^-]_i$ may shift the Eq.1 to the right in c-hNECs perfused with Zero-CO_2. We also examined the effects of an NH_4^+ pulse on CBF and pH_i in c-hNECs perfused with the control solution (5% CO_2). The application of NH_4^+ pulse immediately increased the CBF and pH_i and then gradually decreased them. The cessation of NH_4^+ pulse immediately decreased the CBF and pH_i (Figure 6B,C). The pH_i was 7.55 in c-hNECs perfused with the control solution, and the values of pH_i at 1 min and 7 min from the start of the NH_4^+ pulse were 8.08 and 7.65, respectively ($n = 9$, $p < 0.05$), indicating that H^+ is produced during the application of NH_4^+ pulse in c-hNECs perfused with the control solution. The application of NH_4^+ pulse increased the pH_i, with the high pH_i appearing to shift the Eq. 1 to the right.

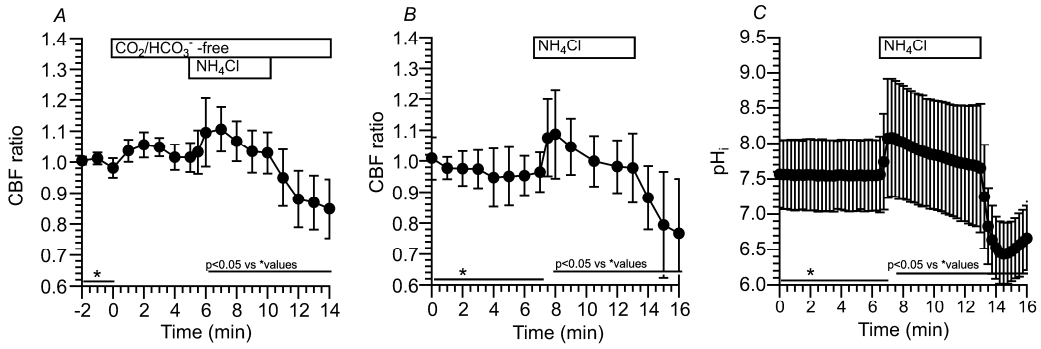

 doi:10.20944/preprints202406.2013.v1

Figure 6. Changes in CBF and pH_i induced by an NH_4^+ pulse in c-hNECs. **(A)** Changes in CBF upon applying an NH_4^+ pulse in the Zero-CO_2. The application of Zero-CO_2 slightly increased the CBF, but its increase was not significant. The NH_4^+ pulse induced an immediate increase followed by a gradual decrease in CBF. The cessation of NH_4^+ pulse immediately decreased the CBF. **(B)** Changes in CBF induced by the NH_4^+ pulse in the control solution. The application of NH_4^+ pulse induced an immediate increase followed by a gradual decrease in CBF. Cessation of the NH_4^+ pulse immediately decreased the CBF. **(C)** Changes in pH_i upon applying the NH_4^+ pulse. The NH_4^+ pulse induced an immediate increase followed by a gradual decrease in pH_i. Cessation of the NH_4^+ pulse immediately decreased the pH_i, and the pH_i then gradually increased to the control level.

2.3.1.3. Effects of CA Inhibitors on CBF and pH_i Changed by Applying the CO_2/HCO_3^--Free Solution and NH_4^+ Pulse in c-hNECs

The addition of dorzolamide (1 μM, an inhibitor of CAII and CAIV) did not change the CBF ratio. The subsequent application of Zero-CO_2 did not change the CBF ratio (Figure 7A). The CBF ratio was 0.98 (n = 16) at 5 min after the addition of dorzolamide and 0.99 at 5 min after the application of Zero-CO_2. The effects of brinzolamide (0.1 μM, a CAII inhibitor) on CBF were also examined. The addition of brinzolamide and the subsequent application of Zero-CO_2 did not change the CBF ratio (Figure 7B). The CBF ratio was 1.00 (n = 21) at 5 min after the addition of brinzolamide and 0.98 at 5 min after the application of Zero-CO_2. In the presence of brinzolamide, the NH_4^+ pulse was applied. The addition of brinzolamide did not change the CBF in c-hNECs, and the subsequent application of NH_4^+ pulse induced an immediate increase followed by a gradual increase in CBF. The CBF ratio was 1.07 (n = 7) at 1 min from the start of the NH_4^+ pulse and 1.17 at 5 min from the start of the NH_4^+ pulse. Cessation of the NH_4^+ pulse immediately decreased the CBF (Figure 7C). In the presence of brinzolamide, the application of NH_4^+ pulse increased the CBF without any CBF decrease. We also measured the pH_i during the application of the NH_4^+ pulse. Brinzolamide did not affect the pH_i. The values of pH_i were 7.81 (n = 6) before and 7.69 at 5 min after the addition of brinzolamide. The application of NH_4^+ pulse increased and plateaued the pH_i, and the pH_i was 8.46 (n = 6) at 1 min and 8.41 at 5 min from the start of the NH_4^+ pulse. Cessation of the NH_4^+ pulse decreased the pH_i (Figure 7D). The effects of dorzolamide on CBF were similar to those of brinzolamide upon applying the CO_2/HCO_3^--free solution or the NH_4^+ pulse. Brinzolamide and dorzolamide similarly inhibit the Eq.1 in c-hNECs, although CAII is a cytosolic enzyme and CAIV is a secreted enzyme. CAIV is suggested to interact with CAII.

 doi:10.20944/preprints202406.2013.v1

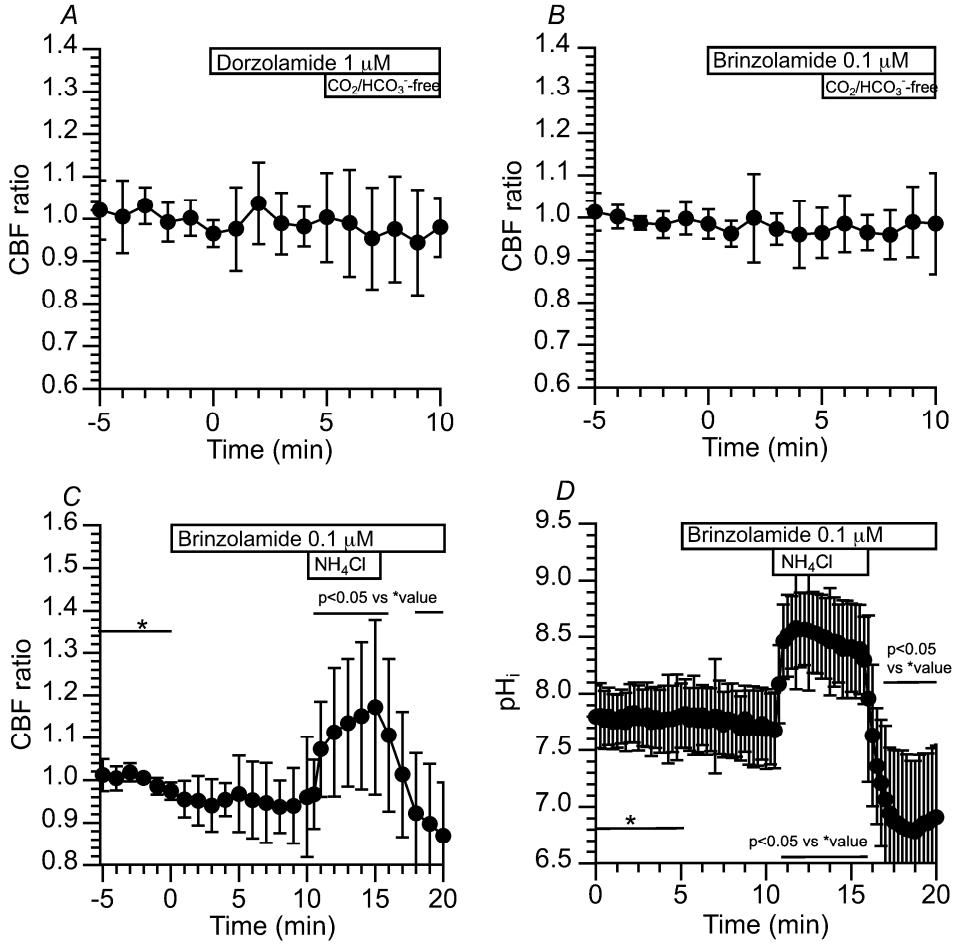

Figure 7. Effects of dorzolamide (an inhibitor of CAII and CAIV) and brinzolamide (a selective inhibitor of CAII) on CBF and pH_i in c-hNECs. **(A)** Effects of dorzolamide (1 μM) on CBF upon applying Zero-CO_2. Dorzolamide abolished the CBF decrease induced by applying Zero-CO_2. **(B)** Effects of brinzolamide (0.1 μM) on CBF upon applying Zero-CO_2. The addition of brinzolamide abolished the CBF decrease induced by applying the CO_2/HCO_3^--free solution. **(C)** Effects of brinzolamide on CBF changes induced by the NH_4^+ pulse. In the presence of brinzolamide, the application of NH_4^+ pulse induced an immediate increase followed by a gradual increase in CBF. Brinzolamide induced a gradual increase in CBF, without any decrease, during the NH_4^+ pulse. Cessation of the NH_4^+ pulse immediately decreased the CBF. **(D)** Effects of brinzolamide on pH_i changes induced by the NH_4^+ pulse. Brinzolamide alone did not change the pH_i. The subsequent application of NH_4^+ pulse induced an immediate increase followed by a slight decrease in pH_i. Cessation of the NH_4^+ pulse immediately decreased the pH_i, and the pH_i then increased gradually to a control value.

2.3.1.4. Effects of NBC Inhibitors (S0859 and DIDS) on CBF and pH_i in c-hNECs

A high pH_i appears to be produced by the HCO_3^- entry in c-hNECs. To inhibit NBC, S0859 (30 μM, a selective inhibitor of NBC) was used. The addition of S0859 decreased the CBF ratio from 1.00 to 0.79 (n = 9, at 5 min after the S0859 addition). Removing S0859 recovered the CBF ratio to 0.99 (at 1 min after removing S0859) (Figure 8A). Experiments were also carried out using DIDS (200 μM, an inhibitor of NBC) (Figure 8B). The addition of DIDS, similarly to S0859, decreased the CBF ratio from 0.99 to 0.78 (n = 5, at 5 min after the addition of DIDS). However, the removal of DIDS did not recover the CBF ratio, and the CBF ratio was 0.71 at 5 min after removing DIDS. Thus, the inhibition of NBC decreases pH_i in c-hNECs. Changes in pH_i were measured in c-hNECs. S0859 decreased the pH_i in c-hNECs, and the pH_i value was 7.54 before and 7.45 (n = 10, $p < 0.01$) at 5 min after the addition of

 doi:10.20944/preprints202406.2013.v1

S0859. The removal of S0859 immediately increased the pH_i, which then decreased gradually. The pH_i was 7.60 at 3 min after removing S0859 (Figure 8C).

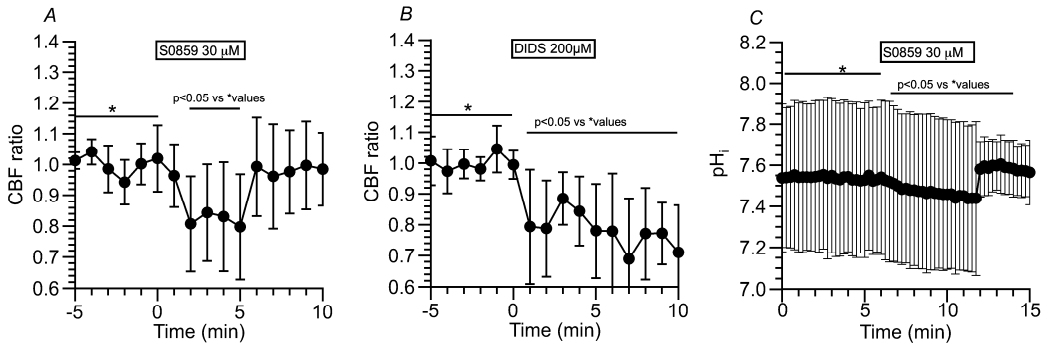

Figure 8. Effects of NBC inhibitors (S0859 and DIDS) on CBF and pH_i in c-hNECs. **(A)** S0859 (30 μM). The addition of S0859 decreased the CBF. The removal of S0859 increased the CBF to a control level. **(B)** DIDS (200 μM). The addition of DIDS decreased the CBF. However, the removal of DIDS did not recover the CBF. **(C)** Effects of S0859 on pH_i. The addition of S0859 gradually decreased the pH_i, the removal of S0859 increased the pH_i, and the pH_i then decreased gradually.

The effects of brinzolamide (0.1 μM) on the decrease in CBF induced by S0859 were examined in c-hNECs (Figure 9A). In the presence of brinzolamide, S0859 did not decrease the CBF ratio. These results suggest that the interactions of CAII, CAIV and NBC may function as the bicarbonate transport metabolon in c-hNECs, as previously reported [21]. The HCO_3^- entry via NBC appears to maintain the high pH_i, which is a key factor for decreasing the CBF and pH_i upon applying Zero-CO_2. We treated c-hNECs with S0859 for 1 h to decrease $[HCO_3^-]_i$. The application of Zero-CO_2 increased the CBF ratio transiently in c-hNECs treated with S0859 (Figure 9B). The CBF ratio was 1.00 (n = 4) before and 1.19 at 3 min after applying Zero-CO_2, suggesting that the application of Zero-CO_2 increased the pH_i in c-hNECs.

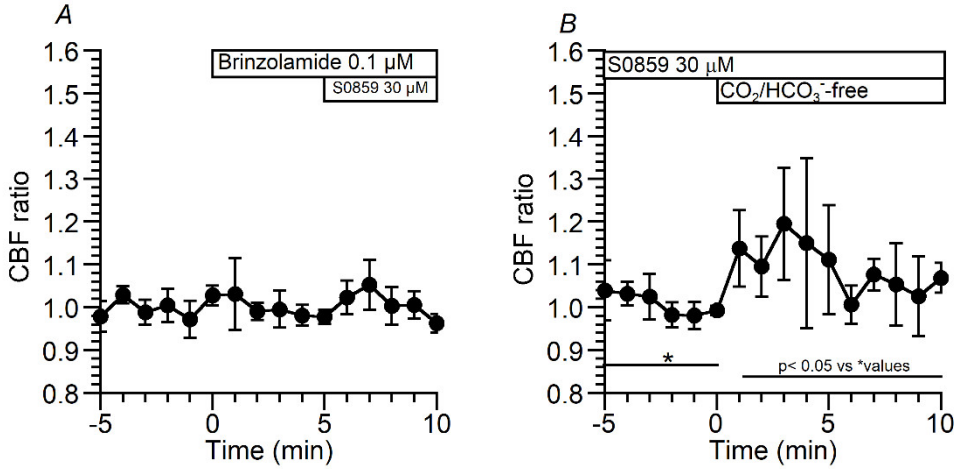

Figure 9. Effects of S0859 on CBF. **(A)** Prior treatment of brinzolamide. In the presence of brinzolamide, the addition of S0859 did not change CBF in c-hNECs. **(B)** The c-hNECs were treated with S0859 for 1 hr. The application of Zero-CO_2 transiently increased the CBF in c-hNECs.

These results suggest that the interactions of CAII, CAIV and NBC accelerate the rate of HCO_3^- influx in c-hNECs. A high rate of HCO_3^- entry through NBC is essential to keep an extremely high pH_i in c-hNECs. Previous studies demonstrated that CAIV plays a key role in maximizing the rate of HCO_3^- transport via NBC in kidney proximal tubules and retinal epithelia [14–16,20,21].

 doi:10.20944/preprints202406.2013.v1

To clarify the role of CAIV in HCO_3^- transport, similar experiments were carried out using c-hBECs expressing no CAIV. Ciliated-hBECs were differentiated from NHBE cells using ALI culture. We measured CBF and pH_i upon applying Zero-CO_2 and the NH_4^+ pulse in c-hBECs.

2.3.2. Ciliated-hBECs

2.3.2.1. Effects of Zero-CO_2 and the NH_4^+ pulse on CBF and pH_i in c-hBECs

Application of Zero-CO_2 transiently increased the CBF and CBD. The CBF and CBD ratios at 2 min after the application were 1.10 (n = 6) and 1.18 (n = 5), respectively (Figure 10A). Changes in pH_i were also measured upon applying Zero-CO_2. The pH_i was 7.10 (n = 10) in c-hBECs perfused with the control solution. The application of Zero-CO_2 transiently increased the pH_i (Figure 10B). Changes in pH_i during the NH_4^+ pulse were also measured. Application of the NH_4^+ pulse increased and plateaued the CBF ratio within 2 min (Figure 10C). Application of the NH_4^+ pulse increased and plateaued the pH_i (Figure 10D). The pH_i before the NH_4^+ pulse was 6.96 (n = 8). The NH_4^+ pulse immediately increased the pH_i, and the pH_i at 5 min from the start of the NH_4^+ pulse was 7.26 (n = 10). Thus, the pH_i of c-hBECs was lower than that of c-hNECs. The application of Zero-CO_2 transiently increased the CBF, and the application of NH_4^+ pulse increased and plateaued the pH_i in c-hBECs (Figure 10).

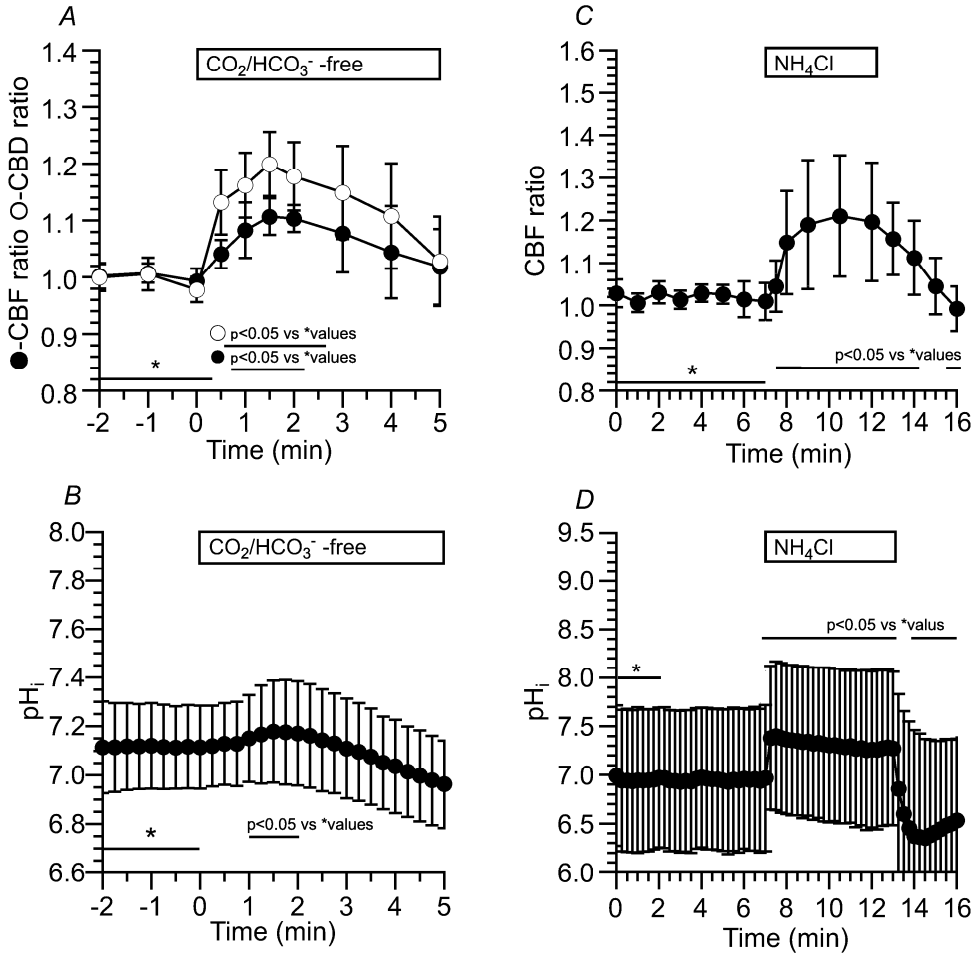

Figure 10. Effects of Zero-CO_2 and the NH_4^+ pulse on CBF, CBD and pH_i in c-hBECs. **(A)** Application of Zero-CO_2 transiently increased the CBF and CBD in c-hBECs. **(B)** Application of Zero-CO_2 transiently increased the pH_i in c-hBECs. **(C)** Application of the NH_4^+ pulse in the control solution increased and plateaued CBF. Cessation of the NH_4^+ pulse decreased the CBF. **(D)** Application of the NH_4^+ pulse immediately increased and plateaued the pH_i without any decrease. Cessation of the NH_4^+ pulse decreased the pH_i and then gradually increased to a control level.

 doi:10.20944/preprints202406.2013.v1

2.3.2.2. Effects of Brinzolamide and S0859 on CBF and pH_i in c-hBECs

Brinzolamide (0.1 μM) gradually decreased the CBF ratio in c-hBECs, suggesting that the left shift of Eq.1 occurred via CAII (conversion to CO_2 from H^+ produced by the cellular metabolism during the control perfusion. Application of the NH_4^+ pulse increased and plateaued the CBF ratio. Cessation of the NH_4^+ pulse immediately decreased the CBF ratio (Figure 11A). Changes in pH_i were measured. The addition of brinzolamide slightly decreased the pH_i (not significant). Application of the NH_4^+ pulse sustained pH_i (Figure 11B). The pH_i values before and 5 min after the brinzolamide addition were 7.43 and 7.38 (n = 5), respectively, and the pH_i at 5 min from the start of the NH_4^+ pulse was 7.77. The addition of S0859 did not change the CBF ratio, but the removal of S0859 gradually increased the CBF ratio (Figure 11C). NBC appears to function in c-hBECs. Changes in pH_i induced by S0859 were measured. S0859 did not change the pH_i, but the removal of S0859 increased the pH_i slightly (Figure 11D). These suggest that pH_i is maintained by interactions of CAII and NBC in c-hBECs, and increases in CBF and pH_i after removing S0859 indicate that HCO_3^- enters cells through NBC during control perfusion. The effects of S0859 on CBF and pH_i indicate that the rate of HCO_3^- influx is much lower in c-hBECs than in c-hNECs.

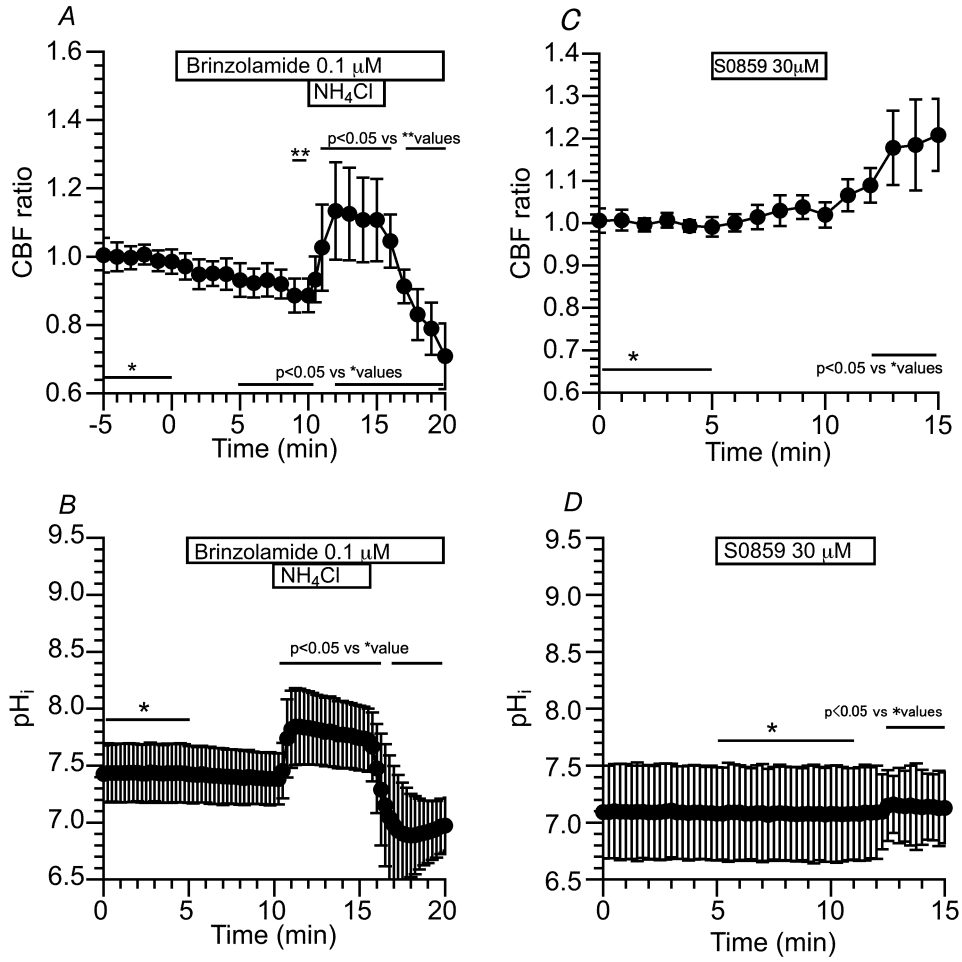

Figure 11. Effects of brinzolamide and S0859 on CBF and pH_i in c-hBECs. **(A)** The addition of brinzolamide gradually decreased the CBF, and then, application of the NH_4^+ pulse increased and plateaued CBF. Cessation of the NH_4^+ pulse decreased the CBF. **(B)** The addition of brinzolamide (0.1 μM) gradually decreased the pH_i, and the NH_4^+ pulse then increased and plateaued the pH_i. Cessation of the NH_4^+ pulse decreased the pH_i. **(C)** The addition of S0859 slightly increased the CBF (not significant). Removing S0859 gradually increased the CBF. **(D)** The addition of S0859 did not change the pH_i. Removing S0859 slightly increased the pH_i.

 doi:10.20944/preprints202406.2013.v1

3. Discussion

The present study demonstrated that the pH_i of c-hNECs is extremely high (7.66) and that the high pH_i is generated by a high rate of HCO_3^- influx in c-hNECs. The $[HCO_3^-]_i$ is calculated to be 41.4 mM from pH_i (7.66) and pCO_2 (5% CO_2, 38 mmHg) using the Henderson–Hasselbalch equation in c-hNECs. This study also demonstrated that the pH_i of c-hBECs is low (7.10) and that the low pH_i is generated by a low rate of HCO_3^- influx. The $[HCO_3^-]_i$ is calculated to be 11.4 mM from the pH_i (7.1) and pCO_2 (38 mmHg) in c-hBECs. The $[HCO_3^-]_i$ of c-hNECs is approximately four times higher than that of c-hBECs.

The high level of pH_i caused a decrease or a small increase in pH_i upon applying Zero-CO_2 in c-hNECs, leading to a decrease or small increase in CBF. Similar results have already been shown in c-hNECs [6]. As shown above, the pH_i and $[HCO_3^-]_i$ were extremely high in c-hNECs in the control solution, and the switch to Zero-CO_2 decreased $[HCO_3^-]_i$ due to there being no HCO_3^- entry. An extremely high pH_i (low $[H^+]_i$) and a low $[HCO_3^-]_i$ appear to shift the Eq.1 to the right (H^+ production) even in the Zero-CO_2, in which a small amount of CO_2 is supplied via cellular metabolism. A decrease in pH_i caused CBF and CBD to decrease in c-hNECs [8,9]. However, in the c-hBECs, the pH_i and $[HCO_3^-]_i$ were low due to there being a low rate of HCO_3^- influx. Under this condition, the switch to Zero-CO_2, which decreases the CO_2 concentration while keeping a low pH_i (a high $[H^+]_i$) and low $[HCO_3^-]_i$, shifts the Eq. 1 to the left to increase the pH_i (CO_2 production from H^+). This pH_i increase enhances CBF and CBD in c-hBECs [8,9]. Thus, an extremely high pH_i is the key factor in shifting the Eq. 1 to the right upon applying Zero-CO_2 in c-hNECs.

The application of Zero-CO_2 appears to induce a large decrease in $[HCO_3^-]_i$ in c-hNECs. The effects of the decrease in $[HCO_3^-]_i$ on Eq.1 may be much larger than those of the decrease in $[CO_2]_i$ in c-hNECS upon applying Zero-CO_2. In c-hBECs, however, the application of Zero-CO_2 decreases $[CO_2]_i$ to an extremely low level and may induce little decrease in $[HCO_3^-]_i$ because of a low HCO_3^- influx rate. The effects of the decrease in $[CO_2]_i$ on the Eq. 1 may be much larger than those of the $[HCO_3^-]_i$ decrease in c-hBECs, inducing the left shift upon applying Zero-CO_2.

The high rate of HCO_3^- transport into cells is maintained in c-hNECs, leading to an extremely high pH_i. RT-PCR analysis revealed that NBC (NBC1, NBCe1, NBCe2, NBCn1 and NDCBE) and AE (SLC4A2 (AE2)) are expressed in both c-hNECs and c-hBECs. The present study demonstrated that NBC blockers (S0859 and DIDS) decrease CBF in c-hNECs, but that they do not change CBF in c-hBECs. Thus, the activity of NBC is high in c-hNECs, but not in c-hBECs. This indicates that the mechanism stimulating NBC activity exists in c-hNECs.

The contribution of AEs to HCO_3^- entry appears to be small because there was no difference in the CBF decrease induced by S0859 or DIDS in c-hNECs. The Na^+/H^+ exchange (NHE) is unlikely to extrude H^+ from c-hNECs because it has been shown to be inactive at pH_i levels higher than 7.4 [22].

The present study demonstrated that CAIV is expressed in c-hNECs, but not in c-hBECs. The expression of CAIV has already been shown in human nasal epithelia [13]. A previous study demonstrated that the physical and functional interactions between CAIV and NBC maximize transmembrane HCO_3^- transport in HEK239 cells transfected with NBC1b and CAIV [14]. The C-terminal tail of CAIV is anchored in the outer surface of the plasma membrane, and a physical interaction between extracellular CAIV and NBC1 occurs via the fourth extracellular loop of NBC1 [14]. In the basolateral membrane of renal proximal tubules, CAIV, which colocalizes with NBC1, increases NBC1 activity [15]. The R14W mutation of CAIV, which has been detected in an autosomal dominant form of retinitis pigmentosa, impairs the pH balance in photoreceptor cells by affecting HCO_3^- influx [16]. These findings suggest that CAIV interacts with NBC to increase the activity of HCO_3^- transport in the c-hNECs. Ciliated-hBECs express HCO_3^- transporters, but no CAIV. A previous report showed that the expression of CAIV was low in the trachea [26]. The NBC blocker study exhibited that the activity of NBC is low in c-hBECs, as described above. Moreover, c-hBECs kept a low pH_i. These indicate that no expression of CAIV causes low NBC activity in c-hBECs. These results indicate that CAIV increases the NBC activity to maximize the rate of HCO_3^- transport into cell in c-hNECs.

 doi:10.20944/preprints202406.2013.v1

CAII has been shown to interact with NBC1 [21,23,26]. CAII and CAIV have similar structures, and the acid motif in the NBC1 C-terminal region interacts with the basic N-terminal region of CAII [21,27]. The HCO_3^-s are produced by CAIV on the apical surface and enter cells via NBCs, and the HCO_3^- in the cells is converted to CO_2 by CAII just below the apical membrane. The coupling of CAIV-NBC-CAII potentiates transmembrane HCO_3^- influxes in c-hNECs [20,21]. In this study, brinzolamide (CAII inhibitor) and dorzolamide (CAII and CAIV inhibitor) showed similar decreases in CBF and pH_i. These results suggest that the interactions of CAIV, NBC and CAIV potentiate the influx of HCO_3^- in c-hNECs. The CAIV, NBC and CAII have been shown to compose the bicarbonate transport metabolon in renal proximal tubules [14,15,20,21]. The c-hNECs also appear to express the bicarbonate transport metabolon consisting of CAIV-NBC-CAII, which maximizes the rate of HCO_3^- transport from the apical surface into the cell.

Kim et al. (2008) showed that eleven CA isozymes are expressed in whole tissue of normal human nasal mucosa using RT-PCR [13]. The activity levels of CAIII and CAXIV are known to be low compared with those of CAI, CAII, CAIV and CAVb [24,25,28]. The present study demonstrated that c-hNECs express mRNA of CAI, CAII, CAIII, CAIV and CAVb, and that CAIV protein, a secreted CA isozyme, is localized on the apical surface including cilia. Brinzolamide (a selective CAII inhibitor) abolished the decreases in CBF and pH_i upon applying Zero-CO_2 and the NH_4^+ pulse. This suggests that CAII is essential for the HCO_3^- transport metabolon in c-hNECs.

The present study does not provide the localization of NBC isoforms in the apical membrane of c-hNECs. However, it has been demonstrated that NBC1 and CAIV have a physical and functional relationship in HEK293 cells transfected with NBC1 and CAIV [14,20,21]. Liu et al. (2022) also showed that NBC functionally exists in apical membranes of mice bronchioles [29]. The present study suggests that NBC1 exists in the apical membrane of c-hNECs, forming the bicarbonate transport metabolon.

The application of Zero-CO_2 induced various responses in CBF and pH_i, either decreases (Figure 5) or small increases (Figure 6A) [7], although it never induced large increases as shown in c-hBECs (Figure 10) or bronchial ciliated cells [9]. Before measuring the CBF or pH_i, c-hNECs with a permeable support filter were kept in the control solution at room temperature. The conditions of c-hNECs were maintained until experimental conditions, such as the time and temperature, affected the pH_i and CBF. Keeping cells at 4° C in air more than 3 hrs, the pH_i decreased by approximately 0.1–0.15, and at this decreased pH_i, the application of Zero-CO_2 induced no changes or slight increases in pH_i and CBF in c-hNECs.

In this study, two types of nasal tissue (uncinate process and nasal polyp) were resected from 16 patients who required surgery for CS. We measured CBF in c-hNECs differentiated from two cell types of nasal epithelia. The CBFs of c-hNECs obtained from two types of nasal tissue were similar. Moreover, c-hNECs obtained from two types of nasal tissue expressed the CAIV mRNA. Kim et al. showed that the expression levels of eleven CA isozymes were decreased by 80–40% in the nasal polyp [13]. However, they examined mRNA expression using whole samples, and the expression of CA isozymes in nasal polyp was weak in the epithelial layer, but weaker or absent in submucosal glands and vascular endothelial cells. We used c-hNECs cultured using ALI, which contain no submucosal gland and no vascular endothelial cells. Based on these observations, CAII and CAIV, at least, express and function in c-hNECs obtained from nasal polyp samples, although the expression level may be lower than in normal nasal epithelia.

We used c-hBECs obtained using ALI culture from NHBEs as a model of human tracheal epithelia. The NHBEs were bought from Lonza (Lot No. 20TL119094). The c-hBECs used appear to provide a good model of tracheal ciliated epithelial cells, although the NHBEs are not the operation sample.

Ciliated-hNECs were cultured in the ALI with 5% CO_2 for more than 4 weeks. The culture condition with 5% CO_2 is different from the asymmetrical gas condition of c-hNECs and c-hBECs in vivo; the apical surface is exposed to the air (0.04% CO_2) periodically and the basolateral membranes are exposed to interstitial fluid saturated with 5% CO_2 (Figure 12). The ALI with 5% CO_2 enhances the HCO_3^- transport into c-hNECs. This unphysiological gas condition appears to increase the pH_i to

Preprints.org (www.preprints.org) | NOT PEER-REVIEWED | Posted: 28 June 2024 doi:10.20944/preprints202406.2013.v1

an extremely high level by maximizing HCO_3^- transport via the bicarbonate transport metabolon CAIV-NBC-CAII (Figure 12A). In c-hBECs that expressed no CAIV, CO_2 that entered the cells is converted to H^+ and HCO_3^- by CAII. The H^+ produced stays in c-hBECs, decreasing the pH_i, while HCO_3^- is secreted to the lumen. Thus, the ALI culture condition may enhance HCO_3^- entry in c-hNECs and CO_2 entry in c-hBECs, leading to a high pH_i in c-hNECs and a low pH_i in c-hBECs.

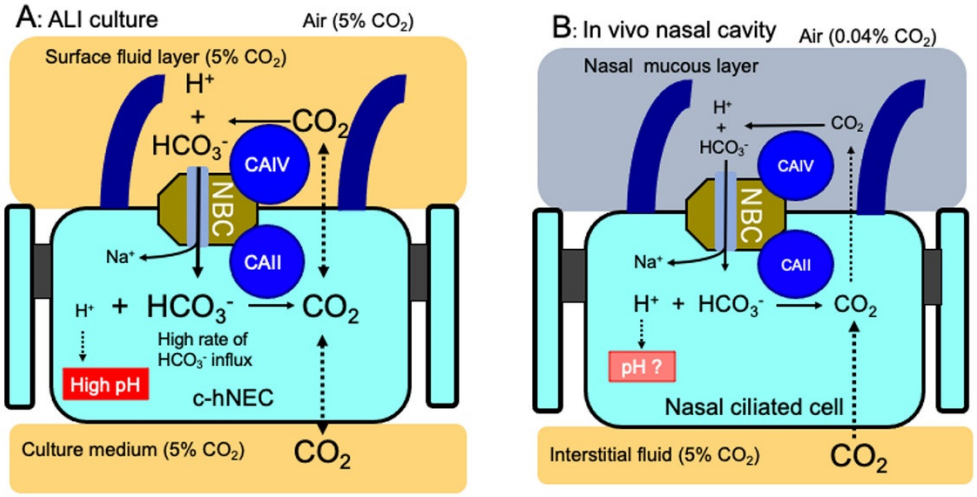

Figure 12. Schematic diagrams of CBF and pH_i regulation by CAIV in c-hNEC (**A**): ALI culture. CO_2 (5%) supplied from the culture gas is converted to HCO_3^- and H^+ by CAIV. The HCO_3^- transport metabolon (CAIV, NBC and CAII) maximizes the rate of HCO_3^- entry in c-hNECs cultured by the ALI. The HCO_3^- entry into cells traps H^+ and is converted to CO_2 by CAII, leading to an extremely high pH_i in c-hNECs. (**B**): In vivo. CO_2, which is leaked from the interstitial fluid (5%) to the apical surface (0.04%), is converted to H^+ and HCO_3^- by CAIV. H^+ stays in the surface mucous layer. The HCO_3^- enters cell via the HCO_3^- transport metabolon. The HCO_3^- that entered the cells, which is removed by CAII, maintains adequate pH_i and CBF levels in c-hNECs exposed to air (0.04% CO_2). At present, we do not know the exact pH_i of c-hNECs in vivo.

In conclusion, we identified a novel bicarbonate transport metabolon consisting of CAIV, NBC and CAII, which regulates pH_i in c-hNECs. In the physiological condition, CO_2 diffuses to the apical surface from the interstitial space according to the CO_2 gradient between interstitial fluid (5%) and air (0.04%). The leaked CO_2 is converted to H^+ and HCO_3^- by CAIV. The HCO_3^- enters cells via NBC, and the H^+ stays in the nasal surface mucous layer, maintaining a low pH. A low pH in the nasal mucous layer is essential for maintaining a healthy nasal cavity capable of, for instance, providing protection from inhaled bacteria [30,31] (Figure 12B). The HCO_3^- that entered the cells is immediately removed by CAII, producing CO_2. The removal of HCO_3^- by CAII enables the continuous transportation of HCO_3^- into the cell by keeping the driving force for HCO_3^- entry. Although we do not know the exact pCO_2 and $[HCO_3^-]_i$ of nasal ciliary cells periodically exposed to air, the HCO_3^- transport metabolon appears to be essential for maintaining pH_i and ciliary beating of c-hNECs at adequate levels in the air. The bicarbonate transport metabolon (CAIV-NBC-CAII), which controls the transmembrane influx of HCO_3^-, appears to be essential for controlling the CBF and pH_i in c-hNECs. Further studies are required to understand this novel mechanism in nasal epithelia in vivo.

4. Materials and Methods

4.1. Ethical Approval

This study has been approved by the ethical committees of the Kyoto Prefectural University of Medicine (RBMR-C-1249-7) and Ritsumeikan University (BKC-HM-2020-090). All experiments were performed in accordance with the ethical principles for medical research outlined in the Declaration of Helsinki (1964) and its subsequent revisions (https://www.wma.net/). Informed consent was obtained from all patients before operation. Human nasal tissue samples (nasal polyp or uncinate

 doi:10.20944/preprints202406.2013.v1

process) were resected from patients who required surgery for chronic sinusitis (16 patients). Samples were immediately cooled and stored in the cooled control solution (4°C) until cell isolation [6].

4.2. Solution and Chemicals

The control solution contained 121 mM of NaCl, 4.5 mM of KCl, 25 mM of $NaHCO_3$, 1 mM of $MgCl_2$, 1.5 mM of $CaCl_2$, 5 mM of NaHEPES, 5 mM of HHEPES and 5 mM of glucose. Its pH was adjusted to 7.4 using HCl (1 M), and the solution was aerated with 95% O_2 and 5% CO_2. The CO_2/HCO_3^--free control solution was prepared by replacing $NaHCO_3$ in the control solution with NaCl and was aerated with 100% O_2. To apply the NH_4^+ pulse, the NaCl (25 mM) in solutions was replaced with NH_4Cl (25 mM). DNase I, amphotericin B, DIDS (4,4-Diisothiocyanatostilbene-2,2-disulfonic acid disodium salt hydrate) and S0859 (a selective NBC inhibitor, 2-chloro-N-((2′-(N-cyanosulfamoyl)-[1,1′-biphenyl]-4-yl)methyl)-N-(4-methylbenzyl) benzamide) were purchased from Sigma-Aldrich (St Louis, MO, USA). Dorzolamide and brinzolamide were purchased from Tokyo Chemical Industry Co., Ltd. (Tokyo, Japan). Can Get Signal® Immunoreaction Enhancer Solution was purchased from TOYOBO (Osaka, Japan).

4.3. Cell Culture Media

Complete PneumaCultTM-Ex Plus medium contained PneumaCultTM-Ex Plus Basal Medium supplemented with PneumaCultTM-Ex supplement (50×, 20 μL/mL), hydrocortisone stock solution (1 μL/mL) and penicillin and streptomycin solution (10 μL/mL). Complete PneumaCultTM-ALI medium contained PneumaCultTM-ALI basal medium supplemented with PneumaCultTM-ALI supplement (10×, 100 μL/mL), PneumaCltTM-ALI maintenance supplement (10 μL/mL), heparin solution (2 μL/mL), hydrocortisone stock solution (2.5 μL/mL) and penicillin/streptomycin solution (10 μL/mL). Solutions and supplements were purchased from STEMCELL Technologies, INC. (Vancouver, BC, Canada). Elastase, bovine serum albumin (BSA) and dimethyl sulfoxide (DMSO) were purchased from FUJIFILM Wako Pure Chemical Corporation (Osaka, Japan). Penicillin/streptomycin mixed solution (penicillin 10000 units/mL and streptomycin 10000 μg/mL in 0.85% NaCl), trypsin, and the trypsin inhibitor were purchased from Nacalai Tesque, Inc. (Kyoto, Japan).

4.4. Antibodies

The anti-CAIV antibody (AF2186, polyclonal goat antibody) was purchased from R&D Systems (Minneapolis, MN, USA). The concentration of MAB2186 used was 1 μg/mL. The antigen peptide (2186-CA, recombinant human CAIV) was also purchased from R&D systems. The anti-alpha-tubulin (acetyl K40) (AC-tubulin) antibody (ab179484) was purchased from Abcam and used at a 100-fold dilution. Alexa Fluor 488 goat anti-mouse IgG (H+L) secondary antibodies (A-11001) and Alexa Fluor 594 donkey anti-rabbit IgG (H+L) secondary antibodies (A-21207) were purchased from Thermo Fischer Scientific (Waltham, MA, USA).

4.5. Cell preparation

We isolated c-hNECs from nasal operation samples as described previously [6]. Briefly, resected samples were cut into small pieces and incubated for 40 min at 37°C in control solution containing elastase (0.02 mg/mL), DNase I (0.02 mg/mL) and BSA (3%). Then, the samples were minced in control solution containing DNase I (0.02 mg/mL) and BSA (3%) using fine forceps. Isolated nasal cells were washed with control solution containing BSA (3%) three times with centrifugation at 160 × *g* for 5 min and then sterilized for 15 min using amphotericin B (0.25 μg/mL) in Ham's F-12 with L-glutamine. Isolated nasal epithelial cells were cultured in complete PneumaCult-Ex medium in a collagen-coated flask (Corning, 25cm^2, NY 14831 USA) at 37°C in a humidified 5% CO_2 atmosphere. The medium was changed every second day. Once the cells reached confluency, they were washed with PBS (5 mL) and harvested in Hank's balanced salt solution (HBSS, 2 mL) containing 0.1 mM EGTA and 0.025% trypsin to remove cells from the flask. Then, a trypsin inhibitor was added into the cell suspension to

 doi:10.20944/preprints202406.2013.v1

stop further digestion. After washing with centrifugation, cells were resuspended in complete PneumaCultTM-Ex Plus medium (1–2 × 10^5 cells, 3mL) and seeded on a filter of a Transwell permeable support insert (Coster 3470, 6.5 mm Transwell with 0.4 μm Pore Polyester Membrane Inserts, Corning) (3.0 × 10^4 cells/insert, 400 μL). Complete PneumaCultTM-Ex Plus medium was added into the upper and bottom chambers and cells were cultured until confluent. Then, the medium in the bottom chamber was replaced with complete PneumaCultTM-ALI medium (500 μL) and the medium in the upper chamber was removed to expose cells to the air (ALI culture). The medium in the bottom chamber was changed three times a week. Cells were cultured for 4 weeks under the ALI condition to allow differentiation into ciliated cells [6].

NHBE cells were purchased from Lonza (LOT No. 20TL119094, Basel, Switzerland) and cultured in the flask, in which complete PneumaCultTM-Ex Plus medium was added at 37°C in a humidified 5% CO_2 atmosphere. Once the cells had reached confluency, they were washed with PBS (5 mL) and harvested with HBSS (2 mL) containing 0.1 mM EGTA and 0.025% trypsin. Then, a tripsin inhibitor was added. After washing cells with centrifugation, cells were resuspended in complete PneumaCultTM-Ex Plus medium (3 mL). The cells were seeded onto the filter of Transwell permeable support inserts (3.0 × 10^4 cells/insert, 400 μL) and cultured into complete PneumaCultTM-Ex Plus medium, which was also added to the upper and bottom chambers. Once the cells reached confluency, the medium in the bottom chamber was replaced with PneumaCultTM-ALI medium (500 μL) and the medium in the upper chamber was removed (ALI culture). The medium in the bottom chamber was changed three times a week. Cells were cultured for 3 weeks under the ALI condition [22]. There were no differences in the development of cilia between nasal epithelial and NHBE cells.

4.6. Measurements of CBF and CBD

The insert membrane filter, on which cells had grown, was cut into 4–6 pieces. A piece of membrane with cells was placed on a coverslip precoated with neutralized Cell-Tak (Becton Dickinson Labware, Bedford, MA, USA). The coverslip with cells was then set in a perfusion chamber (20 μL), which was mounted on an inverted microscope (T-2000, NIKON, Tokyo, Japan) connected to a high-speed camera (IDP-Express R2000, Photron Ltd., Tokyo) (high-speed video microscope). The cells were perfused at a constant rate (200 μL/min). Since CBF is sensitive to temperature, the experiments were carried out at 37°C [5–7,9,10]. Video images were recorded for 2 s at 500 fps using a high-speed video microscope. Video images of c-hNECs before and 5 min after applying NH_4^+ pulse are shown in S1 and S2, respectively. The methods to measure CBF and CBD (ciliary bend distance, an index of ciliary beating amplitude (CBA)) have been described in detail [5–7,9,10]. The ratios of CBF (CBF_t/CBF_0) and CBD (CBD_t/CBD_0) were calculated to make comparisons across the experiments. The subscripts '0' and 't' indicate the time from the start of the experiments. Cells with the cut filter were kept in the control solution at room temperature (2–3 hrs) until the start of CBF and CBD measurements. The store conditions, such as temperature and time, affected CBF responses upon Zero-CO_2 application, resulting in a decrease, no change or a small increase, as shown in Figuer 5 and 6.

4.7. Measurement of pH_i

The insert membrane filter with cells was incubated with a Ca^{2+}-free control solution containing 1 mM EGTA (pH 7.2) for 10 min at room temperature, and the cell sheet was then removed from the membrane filter using a fine forceps. Then, the cell sheet was incubated with 2 μM BCECF-AM (Dojindo Laboratories, Kumamoto, Japan) for 30 min at 37°C. After BCECF loading, the cell sheet was cut into small pieces (4–6 pieces) and kept in the control solution at room temperature until pH_i measurements. A piece of cell sheet was set in a perfusion chamber, and the fluorescence of BCECF was measured using an image analysis system (MetaFluor, Molecular Device, USA). BCECF was excited at 440 nm and 490 nm, and the emission was recorded at 530 nm. The fluorescence ratio (F490/F440) was calculated and recorded with the image analysis system. The calibration curve for pH_i was obtained using BCECF-loaded cells perfused with a calibration solution containing nigericin (15 μM, Sigma-Aldrich, St Louis, MO, USA). The pH values of calibration solution were 6.5, 7.0, 7.5,

 doi:10.20944/preprints202406.2013.v1

and 8.0. The calibration solution contained 150.5 mM of KCl, 2 mM of $MgCl_2$, 1 mM of $CaCl_2$, 10 mM of HEPES and 5 mM of glucose.

4.8. RT-PCR

Total RNA samples from c-hNECs and c-hBECs were prepared using an RNeasy Minikit (QIAGEN, Tokyo, Japan). Total RNA was reverse-transcribed to cDNA using an oligo d(T)6 primer and an Omniscript RT kit (QIAGEN). Then, cDNA samples were subjected to Reverse Transcription-Polymerase Chain Reaction (RT-PCR) using KOD FX (TOYOBO). The gene-specific primers for human CA are listed in Table 1, and those for human NBC and anion exchangers (AE) are shown in Table 2. The amplified PCR products were confirmed using agarose gel.

Real-time PCR was performed in c-hNECs and c-hBECs using the cDNA and CAIV primers confirmed using RT-PCR, and the expression levels of CAIV mRNA were quantitatively evaluated. Quantitative analyses for CAIV mRNA expression and GAPDH mRNA expression were performed using the PowerUp SYBR Green Master Mix (Applied Biosystems, Waltham, MA, USA). The expression level of CAIV mRNA was normalized to that of GAPDH.

4.9. Western Blotting

Cells on the insert membrane filter were washed with PBS and removed from the filter. Then, cells were homogenized in a radioimmunoprecipitation assay buffer (50 mM Tris-HCl, 150 mM NaCl, 1% Nonidet-P40, 0.5% sodium deoxycholate and 0.1% SDS, pH 7.6) containing a protease inhibitor cocktail and incubated at 4°C for 20 min. Cells were then centrifuged at 16,000 × *g* for 20 min at 4°C. The supernatant was used as cell lysate. The lysate was incubated at 37°C overnight with PNGase F (Roche, Basel, Switzerland) in PBS containing 15 mM EDTA, 1% Nonidet P-40, 0.2% SDS and 1% 2-mercaptoethanol. Proteins were separated using Laemmli's SDS-polyacrylamide gel electrophoresis (8%–12.5%) and then transferred onto a polyvinylidene difluoride membrane. The membrane was blocked with milk (2.5%) in Tris-buffered saline (10 mM Tris-HCl and 150 mM NaCl, pH 8.5) containing 0.1% Tween 20 (TBST) for 1 h and then incubated with a primary antibody (MAB2186, R&D System) diluted in solution 1 (Can Get Signal Immunoreaction Enhancer Solution, TOYOBO) overnight at 4°C. After washing with TBST, the membrane was incubated with a secondary antibody (AP124P, anti-mouse IgG) diluted in solution 2 (Can Get Signal Immunoreaction Enhancer Solution, TOYOBO) for 1 h at room temperature. After washing, antigen–antibody complexes on the membrane were visualized using a chemiluminescence system (ECL plus; GE Healthcare, Waukesha, WI, USA).

4.10. Immunofluorescence Examination

Immunofluorescence examinations were performed in c-hNECs and c-hBECs [26]. Cells on the Transwell insert membrane filter were removed using a cell scraper and suspended in PBS (2 mL). The cell suspension (0.5 mL) was dropped and dried on the cover slip, to which cells attached. Then, cells were fixed in 4% paraformaldehyde for 30 min and washed three times with PBS containing 10 mM glycine. Cells were permeabilized with 0.1% Triton X-100 for 15 min at room temperature. After 60 min of pre-incubation with PBS containing 3% BSA at room temperature, cells were incubated overnight at 4°C with the anti-CAIV (AF2186) and anti-AC-tubulin (ab179484, Abcam) antibodies. Then, cells were washed with PBS containing 0.1% BSA to remove unbound antibodies. Afterwards, cells were stained with Alexa Fluor 488 goat anti-mouse IgG (H+L) (A-11001, 1:100 dilution) and Alexa Fluor 594 donkey anti-rabbit IgG (H+L) (A-21207, 1:100 dilution) secondary antibodies for 60 min at room temperature. The samples on the coverslip were enclosed with a mounting medium with DAPI (Vector, Burlingame, CA, USA). Cells were observed using a confocal microscope (FV10i, Olympus, Tokyo) [9,10].

4.11. Statistical Analysis

 doi:10.20944/preprints202406.2013.v1

Statistical significance was assessed using one-way analysis of variance or Student's *t*-test (paired or unpaired), as appropriate. Differences were considered significant for *p*-values < 0.05. The results are expressed as the means ± SD.

5. Conclusions

The bicarbonate transport metabolon consisting of CAIV, NBC, and CAII maximized the rate of transmembrane HCO_3^- transport into the cell in c-hNECs. A large amount of HCO_3^- entry in the cells traps H^+, increasing the pH_i to an extremely high level. The high level of pH_i prevents the CBF from increasing upon applying Zero-CO_2. In the physiological condition, the apical surface is periodically exposed to the air (0.04% CO_2) through respiration, while the basolateral membrane faced the interstitial fluid saturated with 5% CO_2. In c-hNECs exposed to the asymmetrical CO_2 condition, the bicarbonate transport metabolon appears to be essential for keeping an adequate pH_i and ciliary beating.

Author Contributions: Conceptualization, T.N. and M.Y.; methodology, S.O., Ta.I., K.K., S.A., T.T, S.I., K.A., Y.M. and T.N. validation, Y.M. and T.I.; investigation, S.O., K.K., K.Y., and Y.K.; resources, T.I., Y.M., S.H., and T.N.; data curation, S.O. and T.N.; writing—original draft preparation, S.O. and T.N.; writing—review and editing, T.N., M.Y. and S.O.; supervision, Y.M.; project administration, M.Y., T.N., and Y.M.; funding acquisition, Y.M. All authors have read and agreed to the published version of the manuscript.

Funding: This work was supported by the Japan Society for the Promotion of Science (No. JP18H03182, to YM).

Institutional Review Board Statement: This study has been approved by the ethical committees of the Kyoto Prefectural University of Medicine (RBMR-C-1249-7) and Ritsumeikan University (BKC-HM-2020-090). All experiments were performed according to the ethical principles for medical research outlined in the Declaration of Helsinki (1964) and its subsequent revisions (https://www.wma.net/).

Informed Consent Statement: Informed consents were obtained from all patients before operation. Human nasal tissue samples (nasal polyp or uncinate process) were resected from patients who required surgery for chronic sinusitis and allergic rhinitis. Samples were immediately cooled and stored in cooled control solution (4°C) until cell isolation. Informed consent was obtained from all patients to publish this paper.

Data Availability Statement: The data that support the findings of this study are in the paper itself and no shared data are used in the paper.

Acknowledgments: We would like to express our thanks to the Faculty of Medicine, Osaka Medical and Pharmaceutical University for allowing us to use the HSVM.

Conflicts of Interest: The authors declare no conflict of interest.

References

1. Afzelius, B. A., Cilia-related diseases. *J Pathol* **2004,** *204*, 470-7.
2. Salathe, M., Regulation of mammalian ciliary beating. *Annu Rev Physiol* **2007,** *69*, 401-22.
3. Button, B.; Cai, L. H.; Ehre, C.; Kesimer, M.; Hill, D. B.; Sheehan, J. K.; Boucher, R. C.; Rubinstein, M., A periciliary brush promotes the lung health by separating the mucus layer from airway epithelia. *Science* **2012,** *337*, 937-41.
4. Wanner, A.; Salathé, M.; O'Riordan, T. G., Mucociliary clearance in the airways. *Am J Respir Crit Care Med* **1996,** *154*, 1868-902.
5. Delmotte, P.; Sanderson, M. J., Ciliary beat frequency is maintained at a maximal rate in the small airways of mouse lung slices. *Am J Respir Cell Mol Biol* **2006,** *35*, 110-7.
6. Inui, T. A.; Murakami, K.; Yasuda, M.; Hirano, S.; Ikeuchi, Y.; Kogiso, H.; Hosogi, S.; Inui, T.; Marunaka, Y.; Nakahari, T., Ciliary beating amplitude controlled by intracellular Cl(-) and a high rate of CO(2) production in ciliated human nasal epithelial cells. *Pflugers Arch* **2019,** *471*, 1127-1142.
7. Yasuda, M.; Inui, T. A.; Hirano, S.; Asano, S.; Okazaki, T.; Inui, T.; Marunaka, Y.; Nakahari, T., Intracellular Cl(-) Regulation of Ciliary Beating in Ciliated Human Nasal Epithelial Cells: Frequency and Distance of Ciliary Beating Observed by High-Speed Video Microscopy. *Int J Mol Sci* **2020,** *21*, 4052.
8. Sutto, Z.; Conner, G. E.; Salathe, M., Regulation of human airway ciliary beat frequency by intracellular pH. *J Physiol* **2004,** *560*, 519-32.

 doi:10.20944/preprints202406.2013.v1

9. Saito, D.; Suzuki, C.; Tanaka, S.; Hosogi, S.; Kawaguchi, K.; Asano, S.; Okamoto, S.; Yasuda, M.; Hirano, S.; Inui, T.; Marunaka, Y.; Nakahari, T., Ambroxol-enhanced ciliary beating via voltage-gated Ca(2+) channels in mouse airway ciliated cells. *Eur J Pharmacol* **2023,** *941*, 175496.
10. Nakahari, T.; Suzuki, C.; Kawaguchi, K.; Hosogi, S.; Tanaka, S.; Asano, S.; Inui, T.; Marunaka, Y., Ambroxol-Enhanced Frequency and Amplitude of Beating Cilia Controlled by a Voltage-Gated Ca(2+) Channel, Cav1.2, via pH(i) Increase and [Cl(-)](i) Decrease in the Lung Airway Epithelial Cells of Mice. *Int J Mol Sci* **2023,** *24*, 16976.
11. Nguyen, T. N.; Koga, Y.; Wakasugi, T.; Kitamura, T.; Suzuki, H., TRPA1/M8 agonists upregulate ciliary beating through the pannexin-1 channel in the human nasal mucosa. *Mol Biol Rep* **2023,** *50*, 2085-2093.
12. Tarun, A. S.; Bryant, B.; Zhai, W.; Solomon, C.; Shusterman, D., Gene expression for carbonic anhydrase isoenzymes in human nasal mucosa. *Chem Senses* **2003,** *28*, 621-9.
13. Kim, T. H.; Lee, H. M.; Lee, S. H.; Kim, H. K.; Lee, J. H.; Oh, K. H.; Lee, S. H., Down-regulation of carbonic anhydrase isoenzymes in nasal polyps. *Laryngoscope* **2008,** *118*, 1856-61.
14. Alvarez, B. V.; Loiselle, F. B.; Supuran, C. T.; Schwartz, G. J.; Casey, J. R., Direct extracellular interaction between carbonic anhydrase IV and the human NBC1 sodium/bicarbonate co-transporter. *Biochemistry* **2003,** *42*, 12321-9.
15. Tsuruoka, S.; Swenson, E. R.; Petrovic, S.; Fujimura, A.; Schwartz, G. J., Role of basolateral carbonic anhydrase in proximal tubular fluid and bicarbonate absorption. *Am J Physiol Renal Physiol* **2001,** *280*, F146-54.
16. Yang, Z.; Alvarez, B. V.; Chakarova, C.; Jiang, L.; Karan, G.; Frederick, J. M.; Zhao, Y.; Sauvé, Y.; Li, X.; Zrenner, E.; Wissinger, B.; Hollander, A. I.; Katz, B.; Baehr, W.; Cremers, F. P.; Casey, J. R.; Bhattacharya, S. S.; Zhang, K., Mutant carbonic anhydrase 4 impairs pH regulation and causes retinal photoreceptor degeneration. *Hum Mol Genet* **2005,** *14*, 255-65.
17. Lee, S. H.; Park, J. H.; Jung, H. H.; Lee, S. H.; Oh, J. W.; Lee, H. M.; Jun, H. S.; Cho, W. J.; Lee, J. Y., Expression and distribution of ion transport mRNAs in human nasal mucosa and nasal polyps. *Acta Otolaryngol* **2005,** *125*, 745-52.
18. Rayner, R. E.; Makena, P.; Prasad, G. L.; Cormet-Boyaka, E., Optimization of Normal Human Bronchial Epithelial (NHBE) Cell 3D Cultures for in vitro Lung Model Studies. *Sci Rep* **2019,** *9*, 500.
19. Schwartz, G. J.; Kittelberger, A. M.; Barnhart, D. A.; Vijayakumar, S., Carbonic anhydrase IV is expressed in H(+)-secreting cells of rabbit kidney. *Am J Physiol Renal Physiol* **2000,** *278*, F894-904.
20. Sterling, D.; Alvarez, B. V.; Casey, J. R., The extracellular component of a transport metabolon. Extracellular loop 4 of the human AE1 Cl-/HCO3- exchanger binds carbonic anhydrase IV. *J Biol Chem* **2002,** *277*, 25239-46.
21. McMurtrie, H. L.; Cleary, H. J.; Alvarez, B. V.; Loiselle, F. B.; Sterling, D.; Morgan, P. E.; Johnson, D. E.; Casey, J. R., The bicarbonate transport metabolon. *J Enzyme Inhib Med Chem* **2004,** *19*, 231-6.
22. Wakabayashi, S.; Hisamitsu, T.; Pang, T.; Shigekawa, M., Kinetic dissection of two distinct proton binding sites in Na+/H+ exchangers by measurement of reverse mode reaction. *J Biol Chem* **2003,** *278*, 43580-5.
23. Gross, E.; Pushkin, A.; Abuladze, N.; Fedotoff, O.; Kurtz, I., Regulation of the sodium bicarbonate cotransporter kNBC1 function: role of Asp(986), Asp(988) and kNBC1-carbonic anhydrase II binding. *J Physiol* **2002,** *544*, 679-85.
24. Lehtonen, J.; Shen, B.; Vihinen, M.; Casini, A.; Scozzafava, A.; Supuran, C. T.; Parkkila, A. K.; Saarnio, J.; Kivelä, A. J.; Waheed, A.; Sly, W. S.; Parkkila, S., Characterization of CA XIII, a novel member of the carbonic anhydrase isozyme family. *J Biol Chem* **2004,** *279*, 2719-27.
25. Supuran, C. T.; Scozzafava, A., Carbonic anhydrases as targets for medicinal chemistry. *Bioorg Med Chem* **2007,** *15*, 4336-50.
26. Sugiura, Y.; Oishi, M.; Amasaki, T.; Soeta, S.; Ichihara, N.; Nishita, T.; Murakami, M.; Amasaki, H.; Asari, M., Immunohistochemical localization and gene expression of carbonic anhydrase isoenzymes CA-II and CA-VI in canine lower airways and lung. *J Vet Med Sci* **2009,** *71*, 1525-8.
27. Lesburg, C. A.; Huang, C.; Christianson, D. W.; Fierke, C. A., Histidine --> carboxamide ligand substitutions in the zinc binding site of carbonic anhydrase II alter metal coordination geometry but retain catalytic activity. *Biochemistry* **1997,** *36*, 15780-91.
28. Uchida, K.; Okazaki, K.; Nishi, T.; Uose, S.; Nakase, H.; Ohana, M.; Matsushima, Y.; Omori, K.; Chiba, T., Experimental immune-mediated pancreatitis in neonatally thymectomized mice immunized with carbonic anhydrase II and lactoferrin. *Lab Invest* **2002,** *82*, 411-24.
29. Liu, L.; Yamamoto, A.; Yamaguchi, M.; Taniguchi, I.; Nomura, N.; Nakakuki, M.; Kozawa, Y.; Fukuyasu, T.; Higuchi, M.; Niwa, E.; Tamada, T.; Ishiguro, H., Bicarbonate transport of airway surface epithelia in luminally perfused mice bronchioles. *J Physiol Sci* **2022,** *72*, 4.
30. Thornell, I. M.; Li, X.; Tang, X. X.; Brommel, C. M.; Karp, P. H.; Welsh, M. J.; Zabner, J., Nominal carbonic anhydrase activity minimizes airway-surface liquid pH changes during breathing. *Physiol Rep* **2018,** *6*, e13569.

 doi:10.20944/preprints202406.2013.v1

31. Zajac, M.; Dreano, E.; Edwards, A.; Planelles, G.; Sermet-Gaudelus, I., Airway Surface Liquid pH Regulation in Airway Epithelium Current Understandings and Gaps in Knowledge. *Int J Mol Sci* **2021,** *22*, 3384.